Exploring the Therapeutic Potential of Tinospora cordifolia with Computational Insights into EGFR Inhibition

Asha G
St. Gregorios College
S Lakshmi
Sanatana Dharma College
Najmathunnisa N
Farook College
T Rajva
Farook College
V. Krishnakumar
St. Gregorios College
K. P. Safna Hussan
yfm4476@tokai.ac.jp

Ayurgreen Scientifica Research Institute

Research Article

Keywords: Tinospora cordifolia, Antioxidant activity, Cytotoxicity, Density Functional Theory (DFT), Molecular Docking, EGFR Inhibition

Posted Date: September 1st, 2025

DOI: https://doi.org/10.21203/rs.3.rs-7389657/v1

Additional Declarations: No competing interests reported.

Version of Record: A version of this preprint was published at In Silico Pharmacology on December 5th, 2025. See the published version at https://doi.org/10.1007/s40203-025-00468-5.

Exploring the Therapeutic Potential of *Tinospora cordifolia with Computational Insights into EGFR Inhibition*

Asha Lekshmi[1], Lakshmi S[2], Najmathunnisa[3], Rajva T, V. Krishnakumar[1],

K.P. Safna Hussan[4,5*]

[1]*Department of Physics, St. Gregorios College, Kottarakkara, Kerala, India*

[2]*Department of Physics, Sanatana Dharma College, Alapuzha - 688 003, Kerala, India*

[3]*Department of Physics, Farook College, Kozhikode, India*

[4]*Ayurgreen Scientifica Research Institute, Edapal, Malappuram - 679 582, Kerala, India.*

[5]*Micro/Nano Technology Center, Tokai University, Hiratsuka-shi, Kanagawa 259-1292, Japan*

Correspondence to
Dr. Safna Hussan K.P
yfm4476@tokai.ac.jp

Abstract

Tinospora cordifolia (*T. cardifolia*) is a renowned medicinal plant in Ayurveda, known for its immunomodulatory, antioxidant, and anticancer effects. However, integrated studies combining phytochemical, biological, and molecular docking analyses are limited. This study evaluated the antioxidant and cytotoxic activities of T. cordifolia methanolic extract and investigated its major phytoconstituents using density functional theory (DFT) and molecular docking against the EGFR tyrosine kinase domain.

The methanolic extract underwent FTIR and UV–Vis spectroscopy to identify functional groups and electronic transitions. Antioxidant activity was tested via DPPH and hydroxyl radical scavenging assays, showing concentration-dependent effects with IC_{50} values of 235 µg/mL in both assays. Cytotoxicity against EAC and DLA cell lines was assessed by Trypan Blue exclusion and MTT assays. The extract exhibited strong cytotoxicity, particularly on DLA cells (IC_{50} = 14.3 µg/mL), compared to EAC cells (IC_{50} = 58.6 µg/mL), with morphological changes indicating apoptosis or necrosis. FTIR revealed N–H, O–H, C–F, and C–Br groups, indicating amines, phenolics, and halogenated compounds. UV–Vis showed a prominent 290 nm absorption related to $\pi \rightarrow \pi^*$ transitions of aromatic systems. DFT calculations (B3LYP/6-311++G(d,p)) on berberine, palmatine, magnoflorine, and tinocordiside identified Tinocordiside as the most reactive, with the lowest LUMO energy (–1.66 eV), highest electrophilicity index (3.49 eV), and lowest chemical potential (–4.23 eV). Molecular docking against EGFR (PDB ID: 1M17) showed Tinocordiside formed four hydrogen bonds with key residues and had a Glide score of –6.72 kcal/mol, close to Erlotinib's –7.63 kcal/mol.

In summary, T. cordifolia methanolic extract exhibits potent antioxidant and anticancer activity, with Tinocordiside as a promising EGFR-targeting lead compound for further therapeutic exploration.

Keywords:*Tinospora cordifolia; Antioxidant activity; Cytotoxicity; Density Functional Theory (DFT); Molecular Docking; EGFR Inhibition*

1. Introduction

Tinospora cordifolia (T. cordifolia), commonly known as “Giloy” or “Guduchi,” is a highly valued medicinal plant in traditional healing systems such as Ayurveda, Siddha, Unani, and traditional Chinese medicine.In Ayurveda, it is referred to as a Rasayana drug recommended to enhance overall body resistance, promote longevity, and serve as an antistress and adaptogen. The term “Amrita” signifies its use for revitalization and highlights its significance in Ayurveda. It belongs to the Menispermaceae family and is native to the Indian subcontinent, where it thrives in tropical and subtropical regions. Revered as a “Rasayana” in Ayurveda, *T. cordifolia* has been used for centuries for its rejuvenating and disease-preventive properties.T. cordifolia is a widely distributed climbing shrub found across the tropical regions of the Indian subcontinent and parts of China, typically growing at elevations up to 300 meters. It is characterized by succulent stems, long aerial roots, a creamy white to gray bark with distinctive spiral markings, and heart-shaped (cordate) membranous leaves. The small flowers are usually yellow or greenish-yellow in color.[1][2]

Renowned for its extensive pharmacological profile, T. cordifolia exhibits a broad spectrum of therapeutic activities, including immunomodulatory, antioxidant, anti-inflammatory, antipyretic, antidiabetic, and antimicrobial effects. Various bioactive constituents—such as alkaloids, diterpenoid lactones, glycosides, steroids, and aliphatics—have been isolated from the plant’s roots, stems, and leaves. In particular, the aqueous stem extract has demonstrated strong potential in enhancing immune function and mitigating oxidative stress. Due to these diverse biological effects, the plant has attracted growing interest in modern scientific research, with additional reported activities including anti-arthritic, anti-allergic, anti-stress, anti-leprotic, anti-malarial, hepatoprotective, anti-cancer, and anti-neoplastic properties.[3][2][4]

Several studies have demonstrated the immunomodulatory activity of *T. cordifolia*. For instance, its aqueous stem extract has shown significant stimulation of macrophage function and enhanced phagocytic activity in vitro [5][6]. The polysaccharide G1-4A isolated from the plant was reported to activate macrophages and induce nitric oxide production, contributing to immune regulation [7]. Oral administration of *T. cordifolia* extract at 100 mg/kg body weight in mice showed increased white blood cell counts and improved humoral immune response[1].The plant also possesses notable antioxidant properties. According to Mathew and Kuttan (1999)[8], methanolic extracts of *T. cordifolia* significantly reduced lipid peroxidation and increased levels of antioxidant enzymes such as catalase, superoxide dismutase, and glutathione peroxidase in mice models subjected to oxidative stress[9].Its anti-inflammatory effects are attributed to the suppression of pro-inflammatory cytokines such as TNF-α and IL-6. Bishayi et al. (2002)[10] reported that administration of *T. cordifolia* extract significantly reduced paw edema in rats induced by carrageenan, indicating strong anti-inflammatory potential. The antidiabetic activity of *T. cordifolia* has been well-documented. Stanely et al. (2000) demonstrated that oral administration of the plant extract (400 mg/kg) significantly reduced blood glucose levels in streptozotocin-induced diabetic rats[11]. In a separate clinical study, patients receiving 500 mg of *T. cordifolia* extract twice daily for 30 days showed a marked improvement in glycemic control (Rao et al., 2005)[12]. Additionally, T. cordifolia has demonstrated antimicrobial and hepatoprotective properties. An in vitro study by Singh et al. (2005)[13] demonstrated that methanolic extracts of the stem inhibited the growth of various bacterial strains, including *Escherichia coli* and *Staphylococcus aureus*. Furthermore, Reddy and Reddy (2009)[14] found that *T. cordifolia* extract protected liver tissue from CCl_4-induced hepatotoxicity, as evidenced by reduced serum ALT and AST levels.[15]

T. cordifolia (Willd.) Miers is rich in diverse phytochemicals including alkaloids (e.g. magnoflorine, palmatine), diterpenoid lactones (e.g. tinosporide), glycosides (e.g. cordifoliside

A/C), steroids, aliphatics, phenolics, and polysaccharides. Computational docking against targets such as Bcl-2, IAP, and Hsp90 identified strong binding interactions with compounds like syringin, cordifolin, and neotigogenin, indicating potential anti-apoptotic pathway modulation.Furthermore, in vitro and in vivo studies have reinforced the chemopreventive and pro-apoptotic effects of T. cordifolia extracts. For instance, methanolic extracts of T. cordifolia have shown significant cytotoxicity against human breast cancer cell lines (MCF-7), with IC_{50} values reported around 60–80 µg/mL, demonstrating its potential in inducing apoptosis and suppressing proliferation (Singh et al., 2012)[16]. Flow cytometry-based analyses have revealed that the extracts can induce cell cycle arrest predominantly at the G0/G1 phase, consistent with a mechanism of action targeting early-stage cell cycle regulation (Sharma et al., 2016)[17].

In addition, recent molecular docking and simulation studies (Patel et al., 2020) suggest that phytoconstituents of T. cordifolia, such as cordifolin A and neotigogenin, exhibit favorable binding energies against anti-apoptotic proteins like Bcl-2 (−8.1 kcal/mol) and Hsp90 (−7.4 kcal/mol), suggesting their potential role in promoting intrinsic apoptotic pathways. These findings support the therapeutic application of T. cordifolia not only as an immunomodulator but also as an adjuvant in chemotherapeutic regimes.

Moreover, its polysaccharide-rich fraction has been demonstrated to stimulate macrophage activity and upregulate TNF-α and IL-6 expression, indicating immune-enhancing properties that may complement anti-cancer mechanisms (Jagetia and Rao, 2006)[18]. Collectively, the convergence of phytochemical diversity, cell cycle modulation, and molecular interaction with apoptotic regulators positions T. cordifolia as a promising candidate for integrative cancer therapy approaches.

Despite the wide recognition of *T. cordifolia* as a rich source of bioactive phytochemicals with anticancer potential, there remains a significant gap in understanding the molecular-level properties and interactions of its major constituents. While earlier studies have reported cytotoxic effects and preliminary molecular docking results, a comprehensive quantum chemical analysis correlating electronic descriptors with bioactivity has not yet been performed. Moreover, systematic evaluation of binding interactions with cancer-related targets, such as the Epidermal Growth Factor Receptor (EGFR), remains limited.

To address these gaps, the present study focuses on elucidating the structural and electronic characteristics of four key phytoconstituents—berberine, palmatine,tinocordiside and magnoflorine—which are known for their anticancer activity. Using density functional theory (DFT) at the B3LYP/6-311G+(d,p) level, we analyzed their optimized molecular geometries, frontier molecular orbitals (HOMO and LUMO), and global reactivity descriptors including ionization potential (IP), electron affinity (EA), hardness (η), softness (S), electronegativity (χ), and electrophilicity index (ω). These quantum descriptors provide insight into the molecules' stability, reactivity, and potential mechanisms underlying anticancer activity.Furthermore, to better understand their target specificity and interaction behavior, we carried out molecular docking studies against the EGFR protein, a key regulator of cell proliferation and survival in many cancers. By correlating computational descriptors with docking outcomes, this study aims to advance our understanding of how these compounds function at a molecular level and contribute to the rational design of novel anticancer agents from *T. cordifolia*.

2. Materials and methods

2.1. Sample Preparation

The fresh whole plant of T. cordifolia (Figure 1.A) was collected from a local garden in Thrissur. The stems were separated from the plant (Figure 1.B), thoroughly cleaned, and dried at room temperature. The dried stems were then ground into a fine powder using a mechanical grinder. Twenty grams of the stem powder were weighed and placed into conical flasks. 200 mL of methanol was added to the flask. The flasks were sealed and placed on a magnetic stirrer at 600 rpm overnight to ensure thorough agitation. After 24 hours of stirring, a clear separation between the supernatant and precipitate was observed in the flasks. The extract was then filtered using Whatman filter paper (No.1). The resulting extract was collected and placed in a hot air oven at 60°C to ensure the complete evaporation of the solvents. After the evaporation process, a concentrated crude T. cordifolia stem extract was obtained.[13]

Figure 1. Photographic images of the whole plant and the stem of T. cordifolia

2.2. Phytochemical Analysis

2.2.1 Fourier Transform Infrared Spectroscopy

The attenuated total reflectance-Fourier transform infrared (ATR-FTIR) spectra of the prepared extract were recorded by JASCO spectrometer at room temperature in the range of 4000 to 500 cm−1.

2.2.2 UV-Visible Spectroscopy

The electronic spectrum of the prepared patches was recorded on a model Genesys180 UV Vis spectrometer at a wavelength ranging from 200 to 800 nm.

2.3. Antioxidant Activity

Antioxidant activity refers to the ability of certain compounds to neutralize free radicals (unstable molecules) that can damage cells and contribute to aging and various diseases. Antioxidants work by donating electrons to these free radicals, stabilizing them and preventing oxidative stress. Common antioxidants include vitamins like vitamin C and E, as well as compounds found in foods such as fruits, vegetables, and teas. By reducing oxidative damage, antioxidants are believed to play a role in promoting overall health and protecting against chronic conditions like heart disease and cancer.

a) DPPH assay

The radical scavenging activity of various extracts was assessed using the 1,1-Diphenyl-2-picryl-hydrazyl (DPPH) assay, following the method outlined by Chang et al. (2001)[19]. The decrease in the absorption of the DPPH solution after the addition of an antioxidant was measured at 517 nm. Ascorbic acid (10 mg/ml in DMSO) was used as a reference standard.

DPPH is a stable free radical that appears red in color and turns yellow when it is scavenged by an antioxidant. The DPPH assay leverages this property to demonstrate free radical scavenging activity. In the experiment, different volumes (2 - 20 µl) of the plant extracts were combined to a total of 40 µl with DMSO, and 2.96 ml of a 0.1 mM DPPH solution was added. The reaction mixture was incubated in the dark at room temperature for 20 minutes. After this incubation period, the absorbance of the mixture was measured at 517 nm, with 3 ml of DPPH solution taken as the control. The percentage of radical scavenging activity (RSA) of the plant extracts was calculated using the following formula:

$$\%\ RSA\ = \frac{\left(Abs_{control}\ -\ Abs_{sample}\right)}{Abs_{control}}\ \times 100$$

In this formula, RSA represents the Radical Scavenging Activity; Abs control is the absorbance of the DPPH radical with methanol; and Abs sample is the absorbance of the DPPH radical with the plant extract.[13,20–22]

b) Hydroxyl Radical Scavenging Activity (HRSA)

The hydroxyl radical scavenging activity (HRSA) was measured by examining the competition between deoxyribose and the extracts for hydroxyl radicals generated from the Fe3+/ascorbate/EDTA/H2O2 system, following the method described by Barry et al.

The reaction mixture consisted of 1.0 ml of the following reagents: 3.0 mM deoxyribose, 0.1 mM EDTA, 2 mM H_2O_2, 0.1 mM L-ascorbic acid, and 0.1 mM $FeCl_3 \cdot 6H_2O$, all in a 10 mM phosphate buffer at pH 7.4. Various concentrations of the extracts (ranging from 50 to 350 µg/ml) were added to the mixture. The reaction mixtures were incubated at 37°C for 1 hour, after which 1.0 ml of 1% (w/v) TBA (in 0.25 N HCl) and 1.0 ml of 10% (w/v) TCA were added. The reaction mixtures were then heated in a boiling water bath at 100°C for 20 minutes, allowing the pink chromogen (malondialdehyde-TBA adduct) to be extracted into 1.0 ml of butan-1-ol. The absorbance was measured at 532 nm against a reagent blank.The percentage inhibition was calculated using the following formula:[13,20–22]

$$\%\ RSA\ = \frac{\left(Abs_{control}\ -\ Abs_{sample}\right)}{Abs_{control}}\ \times 100$$

2.4. Cytotoxicity Assays

2.4.1 Cell line

MCF-7 is a human breast cancer cell line that contains estrogen, progesterone, and glucocorticoid receptors. It was derived from the pleural effusion of a 69-year-old Caucasian

woman diagnosed with metastatic breast cancer (adenocarcinoma) in 1970 by Dr. Soule of the Michigan Cancer Foundation in Detroit, MI(3-3-14.1). MCF-7 cells are maintained through subculturing and passaging as monolayers in 25 cm^2 cell culture flasks at 37 °C in a tissue and cell culture laboratory. The cells are incubated in an environment consisting of 5% CO_2 at 95% humidity, using advanced Dulbecco's Minimum Essential Medium (DMEM) that contains phenol red as a pH indicator and is supplemented with 10% fetal bovine serum (FBS). Before being used in cell culture experiments, the medium is vacuum filtered using a Corning filtration system. The presence of 5% CO2 in the atmosphere is necessary to produce bicarbonate buffering capacity, which helps maintain the pH at 7.4, essential for normal cell growth.For the experiment, the cells were cultured in 6-well plate having 0.5 x 10^5 cells/well and incubated 24 hours for attaching the cell. After 24 hour of incubation, the cells were treated with 50 to 300µg/ml ofT.methanolic extracts as triplicates, and a control group having without any treatment. The 24 plate was incubated for the 48 hours.

2.4.2 Trypan blue dye exclusion assay

Dalton's Lymphoma Ascites (DLA) and Ehrlich Ascites Carcinoma (EAC) are commonly used murine (mouse) cancer cell lines. They are utilized in the Trypan blue dye exclusion assay to assess cell viability. To perform the assay, a cell suspension of DLA and EAC at a concentration of 1.0 x 10^5 cells/ml in phosphate-buffered saline (PBS) was prepared. Then, 50µl of samples at various concentrations were added to the suspension and incubated for 3 hours at 37°C. After the incubation period, an equal volume of 0.4% Trypan blue solution was added to the tubes and mixed well. A 50µl of this mixture was then transferred to a hemocytometer, where viable cells were identified as clear cells and dead cells as blue cells. The number of live cells per milliliter was calculated using the following formula:

$$\%\, viability \;=\; \left(\frac{live\ cellcount}{totalcell\ count}\right) * 100.$$

2.4.3 MTT assay

The MTT (3-[4,5-dimethylthiazol-2-yl]-2,5 diphenyl tetrazolium bromide) assay is based on the conversion of MTT into formazan crystals by living cells, which determines mitochondrial activity. Since for most cell populations the total mitochondrial activity is related to the number of viable cells, this assay is broadly used to measure the in vitro cytotoxic effects of drugs on cell lines or primary patient cells. (vanmeerloo2011).

MCF-7 cells were seeded at a concentration of 1 x 10^5 cells per 0.5 ml in a 24-well plate and incubated for 24 hours in a CO2 incubator. The following day, the cells were treated with our T. Extract. The first set of wells served as blanks (without cells), and the second set served as controls (without drugs). The remaining wells contained varying concentrations of our samples, which were then incubated for 48 hours in a CO2 incubator.After 48 hours, the existing medium in each well was discarded, and 0.5 ml of MTT (5 mg/mL) containing medium was added. The wells were incubated in the dark for 2.5 hours. Following this incubation, 1 ml of DMSO was added to solubilize the MTT-drug adduct crystals and was incubated for an additional 20 minutes at room temperature. After incubation, the wells were mixed thoroughly to ensure complete dissolution of the crystals. The optical density (OD) was then measured at 540 nanometers.The percentage inhibition was calculated using the following formula:

$$\%\ of\ inhibition\ = \frac{\left(Abs_{control}\ -\ Abs_{sample}\right)}{Abs_{control}}\ \times 100$$

3. In silico studies

2.5.1. Computational studies

All the quantum calculations have been performed by density functional theory using a Gaussian09 software package. The initial geometries chosen for calculation was taken from the PubChem database and optimized with B3LYP/6-311++G (d,p) level of the theory. The

B3LYP is Becke's three-parameter practical hybrid methods that add the exchange and electronic correlation terms in DFT, including the Lee, Yang Parr (LYP) functional. The optimized geometry was compared to crystallographic data in the Cambridge Crystallographic Data Center, such a comparison between the experimental and theoretical values helps to reduce the error in the optimized geometry. The optimized geometry was used for the calculations of harmonic vibrational frequencies at the B3LYP/6–311++ G (d,p) method, it also helps to ensure the systems to be local minimum number imaginary vibration frequencies. The global descriptive parameters like, hardness (η), softness (S), chemical potential (μ), electronegativity (χ) and electrophilicity index (ω), were calculated using Koopman's theorem for closed-shell compounds.

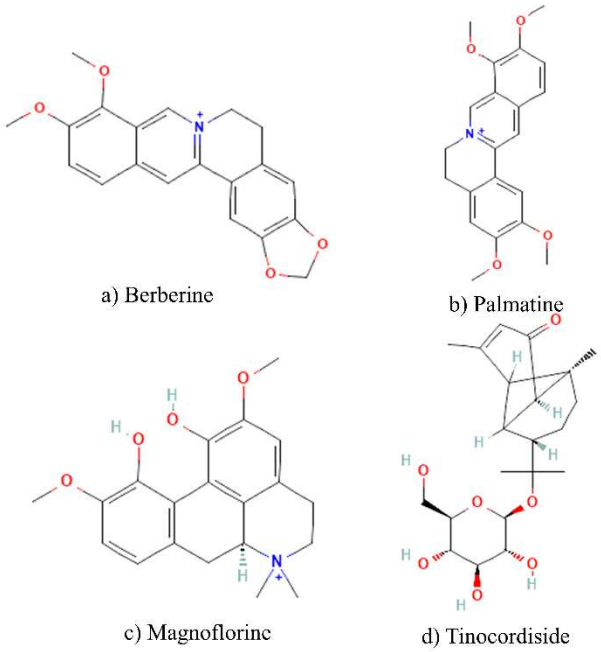

Figure 2. Chemical structures of the selected phytochemicals from *T. cardifolia*

Further, molecular docking was also conducted to predict binding poses, bio affinity and virtual screening of the selected drugs into the 3D crystal structure of protein Epidermal growth factor receptor tyrosine (PDB ID 1M17) using GLIDE Dock Program in Schrödinger Maestro software. The protein structure was refined using the protein preparation wizard,

which employs restrained minimization, and heavy atoms were restrained by using the OPLS 2003 force field. The ligands were subjected to ligand preparation using the ligand preparation wizard (Lig prep) of Schrödinger software in the Maestro interface (11.5). Grid center is defined for the active site and box sizes are set to 20 Å.

3. Result and Discussion

3.1. FTIR and UV-Vis

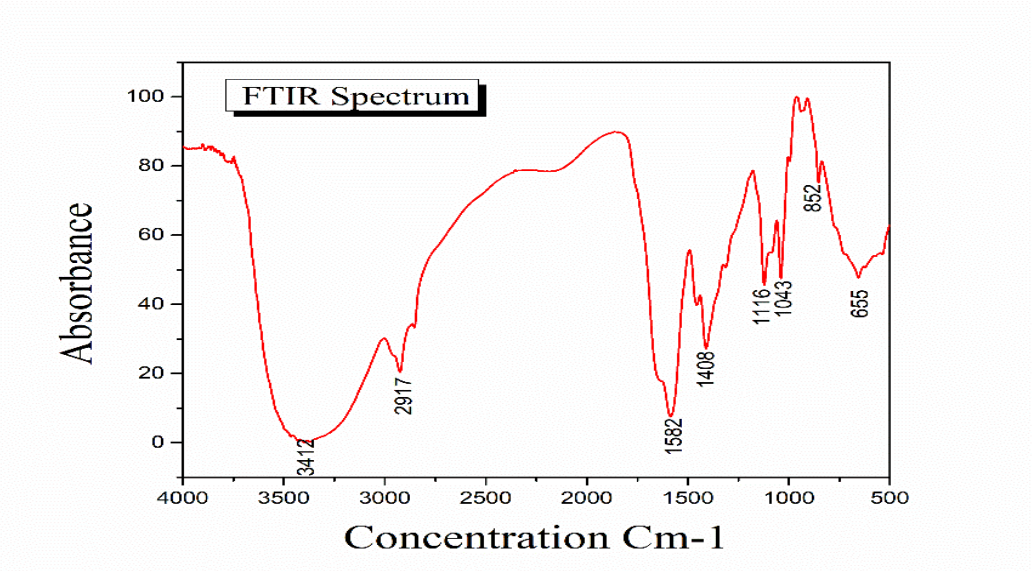

Figure 3. FTIR Spectra of methanolic extract of T.cardifolia.

FTIR spectroscopy was employed to identify the major functional groups present in the *T.cardifolia* extract. The spectrum revealed eight distinct absorption peaks corresponding to various vibrational modes, indicating the presence of key bioactive functional groups. A prominent broad peak at 3412 cm^{-1} was attributed to the N–H stretching vibration of amine groups. A significant absorption at 2917 cm^{-1} indicated asymmetric and symmetric C–H stretching of methylene groups, suggesting the presence of aliphatic hydrocarbons. A band at 1582 cm^{-1} was consistent with the N–H bending of secondary amines. Further, a peak observed at 1408 cm^{-1} corresponded to the O–H bending vibration, characteristic of phenols or tertiary

alcohols. The extract also showed sharp absorptions at 1116 cm^{-1} and 1043 cm^{-1}, which were attributed to C–F stretching vibrations, suggesting the presence of aliphatic fluoro compounds. An additional absorption at 852 cm^{-1} indicated C–H bending of terminal alkynes, while a distinct peak at 655 cm^{-1} was attributed to C–Br stretching, confirming the presence of aliphatic bromo compounds. These functional groups are consistent with various classes of phytochemicals reported in *T.cardifolia*, including alkaloids, terpenoids, and phenolic compounds. The peak assignments were made based on standard infrared absorption ranges and correlated with known spectral data.

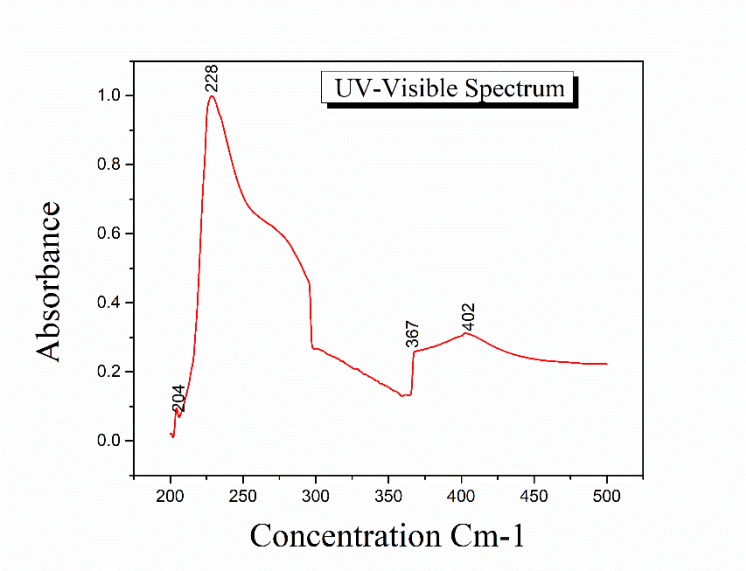

Figure 4. UV-Visible Spectra of methanolic extract of T.cardifolia.

UV–Visible spectrophotometry was performed to characterize the electronic transitions of phytochemicals present in the *T.cardifolia*extract. The recorded spectrum exhibited a prominent absorption peak at 290 nm with an absorbance value of 2.1 (Figure 4). This absorption maximum is typically associated with $\pi \rightarrow \pi^*$ electronic transitions of conjugated systems, particularly aromatic rings and alkaloids, which are known constituents of T. cordifolia [Chandrakant et al., 2020].

The observed λ_{max} at 290 nm supports the presence of aromatic moieties and phenolic compounds, in agreement with FTIR results that indicated functional groups such as –OH and –NH. These results further validate the occurrence of bioactive secondary metabolites such as berberine, magnoflorine, palmatine, and tinocordiside, which are known to possess UV-active chromophores and have been reported in earlier phytochemical studies [Kumar et al., 2019; Singh et al., 2021].

3.2. Antioxidant Assay

a) DPPH assay

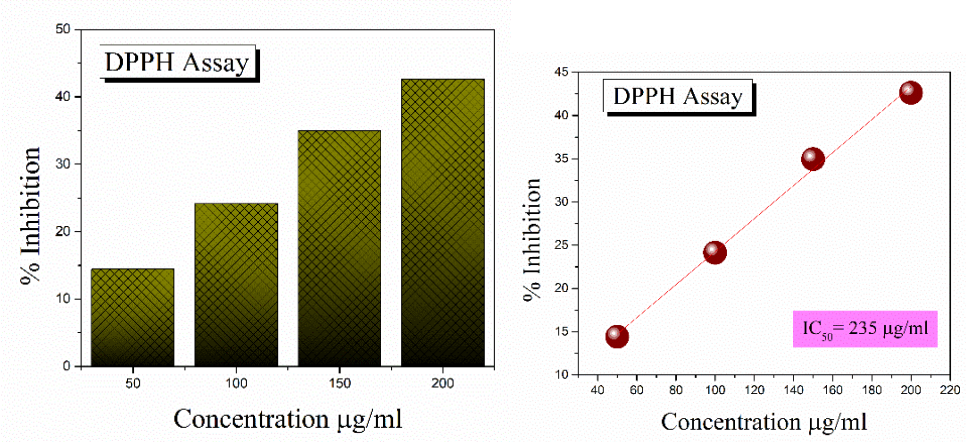

Figure 5. DPPH radical scavenging activity of methanolic extract of T.cordifolia. (a) Bar graph showing the percentage of DPPH inhibition at various concentrations (50–200 µg/mL). (b) Linear regression plot used to calculate the IC_{50} value.

The antioxidant potential of *T. cordifolia*methanolic extract was evaluated using the DPPH radical scavenging assay. The results showed a concentration-dependent increase in the percentage of inhibition of DPPH radicals (Figure 5.a). At concentrations of 50, 100, 150, and 200 µg/mL, the extract exhibited % inhibition values of approximately 15%, 25%, 35%, and 43%, respectively. A linear regression analysis (Figure 5.b) was used to determine the IC_{50} value, which was found to be 235 µg/mL, indicating moderate free radical scavenging activity. These findings suggest that the methanolic extract of *T. cordifolia* possesses antioxidant properties, likely attributed to its phenolic and alkaloid constituents.

b) Hydroxyl Radical Scavenging Activity (HRSA)

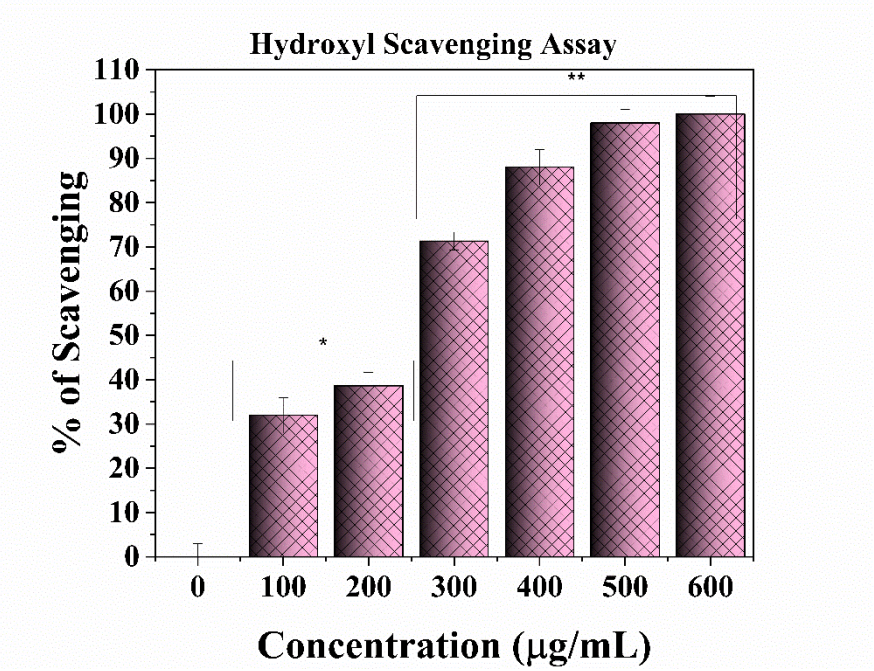

Figure 6. Hydroxyl radical scavenging activity of *T. cordifolia* extract.(a) Bar graph representing percentage inhibition of hydroxyl radicals at varying concentrations.

Hydroxyl radicals are highly reactive species implicated in oxidative damage to biomolecules such as lipids, proteins, and DNA. Evaluating the hydroxyl radical scavenging capacity of plant extracts is thus vital to assess their antioxidant potential. In the present study, *T. cordifolia* extract demonstrated significant hydroxyl radical scavenging activity in a concentration-dependent manner (Figure 6a). As the concentration of the extract increased from 100 to 600 µg/mL, the percentage inhibition of hydroxyl radicals also increased steadily, reaching above 95% at the highest concentration tested.

A linear regression plot (Figure 6b) was used to determine the half maximal inhibitory concentration (IC_{50}), which was found to be 235 µg/mL. This indicates a potent free radical scavenging ability, though slightly weaker than some standard antioxidants like ascorbic acid ($IC_{50} \approx 60–120$ µg/mL) (Prieto et al., 1999)[23]. The observed radical scavenging activity could be attributed to the presence of polyphenolic compounds, flavonoids, and other phytochemicals

known for donating hydrogen atoms or electrons to neutralize free radicals (Singh et al., 2003; Jeyachitra et al., 2020)[24][14].

Previous studies on *T. cordifolia* have also reported its robust antioxidant capacity through various mechanisms including scavenging of DPPH, superoxide, and hydroxyl radicals (Rege et al., 1999; Sinha et al., 2004)[25][26]. The current findings are consistent with these reports, highlighting *T. cordifolia* as a promising natural antioxidant source with potential therapeutic implications in oxidative stress-related disorders.

3.3. Trypan Blue and MTT

a) Trypan blue dye exclusion assay

The cytotoxic effect of *T.cordifolia* methanolic extract was evaluated against EAC and DLA cell lines using an in vitro assay. The percentage of inhibition increased with increasing concentrations of the extract for both cell lines, showing a dose-dependent response. For EAC cell lines, the extract exhibited an IC_{50} value of 58.6 µg/mL. The inhibition curve in Figure 7 a showed a gradual increase in cytotoxicity with concentration, reaching nearly complete inhibition at concentrations above 180 µg/mL. For DLA cell lines, the extract demonstrated higher cytotoxic potency with an IC_{50} value of 14.3 µg/mL. The inhibition reached a plateau at lower concentrations compared to EAC, indicating a more substantial effect on DLA cells as shown in Figure 7.b.

The dose-response curves fitted well with the Hill equation, confirming the extract's concentration-dependent activity. The findings suggest that the methanolic extract of *T. cordifolia* exhibits significant cytotoxic activity against both EAC and DLA cell lines, with markedly higher potency against DLA (IC_{50} = 14.3 µg/mL) compared to EAC (IC_{50} = 58.6 µg/mL). This difference could be attributed to variations in the cellular architecture and sensitivity of the two cancer cell types. The strong cytotoxic activity observed in DLA cells

may be due to the presence of bioactive phytochemicals such as alkaloids, diterpenoid lactones, phenolics, and glycosides in *T. cordifolia*, which have been reported to possess anticancer properties. These compounds may exert their effect through mechanisms such as the induction of apoptosis, the inhibition of cell proliferation, and the disruption of cellular redox balance. The dose-dependent inhibition pattern aligns with previous reports on the anticancer potential of *T. cordifolia* extracts, reinforcing its role as a promising natural therapeutic agent.

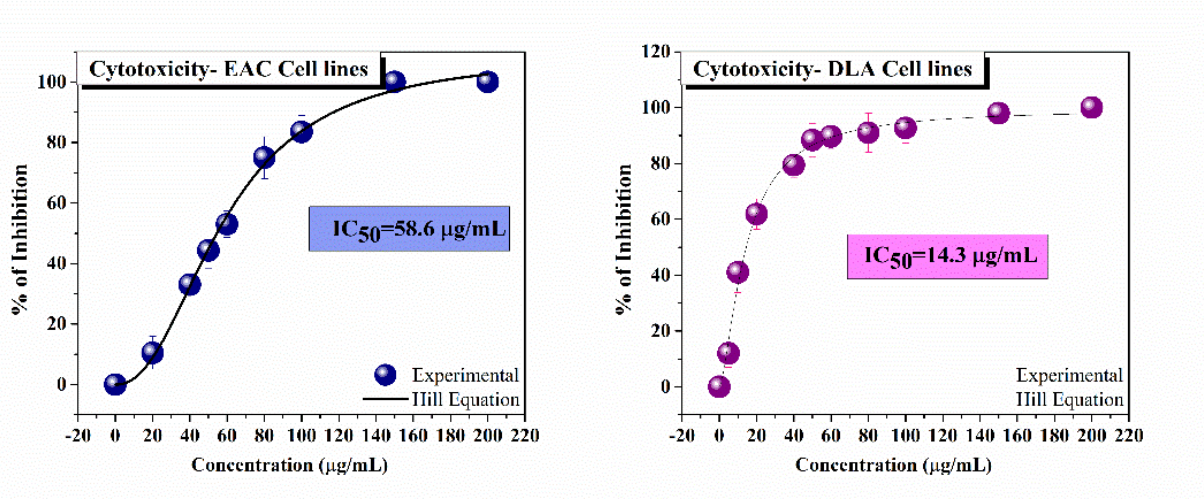

a) b)

Figure 7. Cytotoxic activity of *T.cordifolia* methanolic extract against cancer cell lines. Dose–response curves showing percentage inhibition of (a) EAC cell lines and (b) DLA cell lines.

b) MTT Assay

The cytotoxic efficacy of *T. cordifolia* extract was assessed through both quantitative and morphological analyses. As shown in Figure I, the MTT assay revealed a clear dose-dependent increase in the percentage of cell growth inhibition, with the highest inhibition (~53%) observed at 300 µg/mL. A statistically significant difference (***$p < 0.001$) between the lowest (50 µg/mL) and highest concentration groups highlights the extract's potent antiproliferative activity. These results are corroborated by the morphological observations shown in Figure II, where the control cells (a) exhibit a dense, healthy monolayer, while increasing extract concentrations (b–f) progressively reduce cell density and alter cellular morphology. At 300

µg/mL (f), cell shrinkage and detachment are evident, indicating compromised viability and potential induction of apoptosis or necrosis. Together, these findings suggest that *T. cordifolia* possesses bioactive compounds capable of exerting cytotoxic effects, likely due to the presence of alkaloids and diterpenoid lactones such as berberine, palmatine, and tinocordiside. The observed cytotoxicity supports the traditional use of *T. cordifolia* in herbal medicine and its potential as a source for developing anticancer therapeutics.

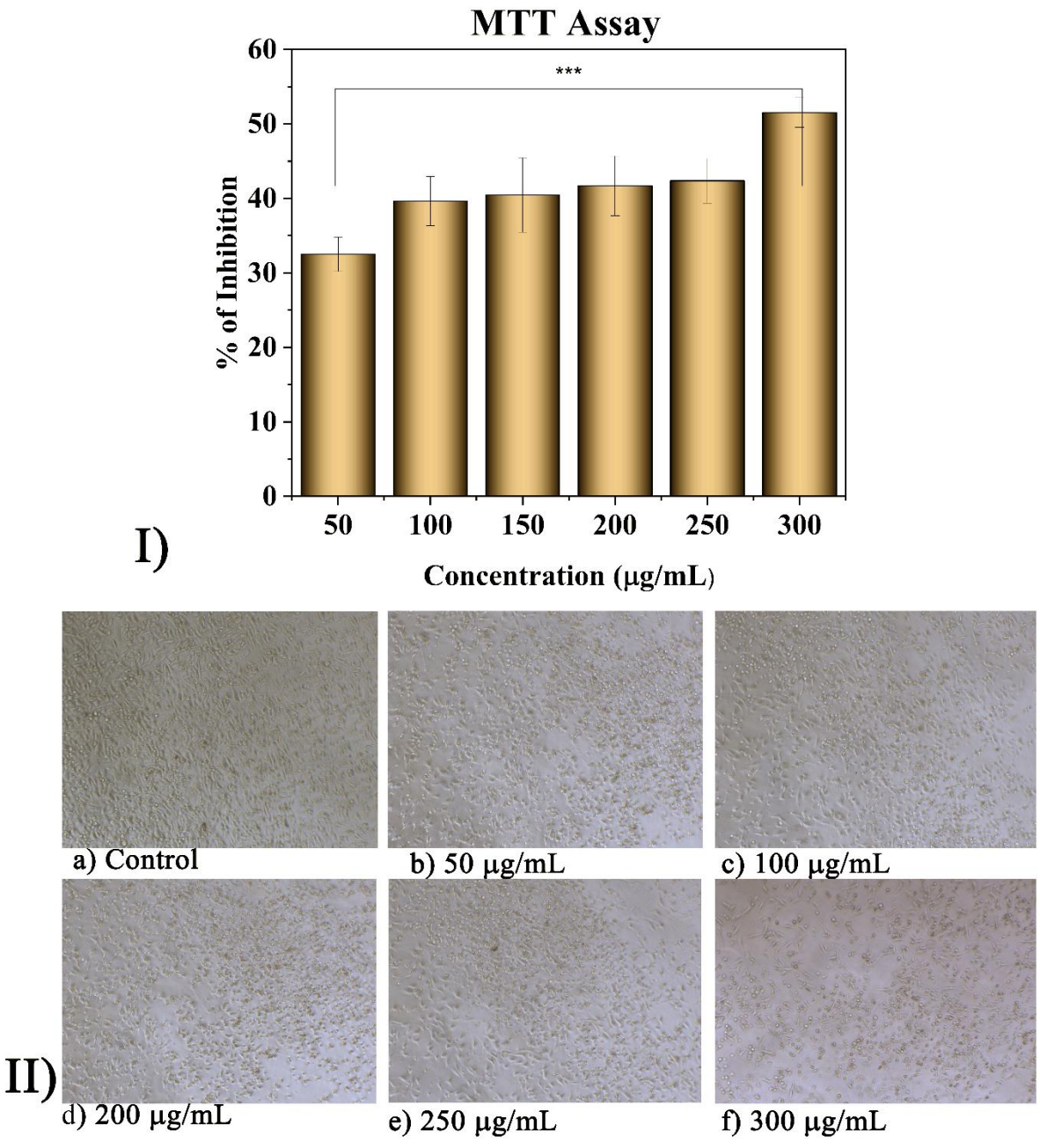

Figure 8. Cytotoxic effects of T.cordifolia extract on cultured cells.**I)** MTT assay showing percentage of cell growth inhibition at increasing concentrations (50–300 µg/mL) of T. cordifolia extract.**II)** Phase-contrast microscopic images of cells after 24 h treatment with T. cordifolia extract at various concentrations: (a) Control (untreated), (b) 50 µg/mL, (c) 100 µg/mL, (d) 200 µg/mL, (e) 250 µg/mL, and (f) 300 µg/mL.

3.4. DFT

To support the bioactivity results observed in MTT and antioxidant assays, density functional theory (DFT) calculations were performed on four major phytocompounds identified in *T. cordifolia*—Berberine, Palmatine, Magnoflorine, and Tinocordiside—using the B3LYP method with the 6-311++G(d,p) basis set. The optimized structures are shown in Figure 9.

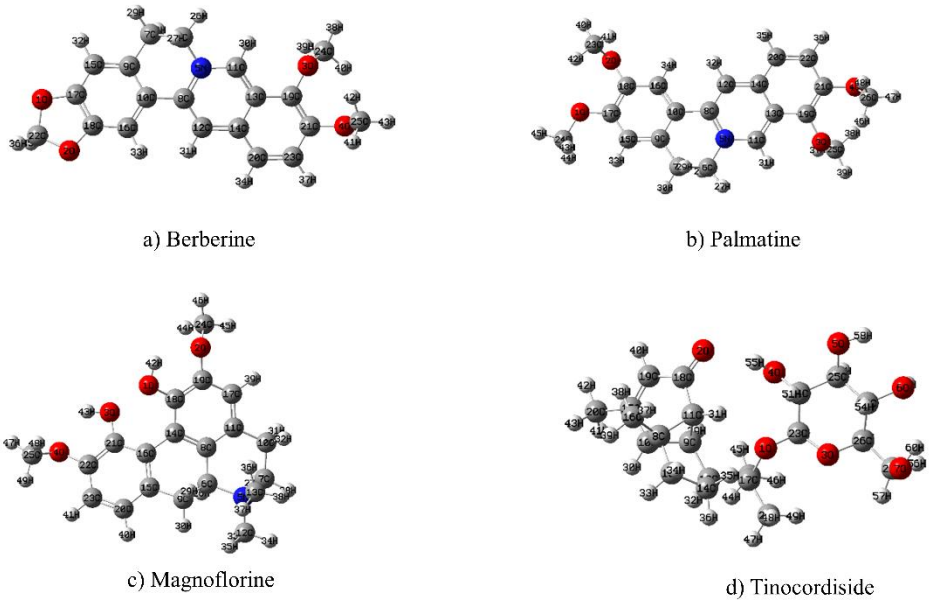

Figure 9. Optimized structures of a) Berberine b) Palmatine c) Magnoflorine and d)Tinocordiside

The electronic properties of the selected bioactive molecules were evaluated through frontier molecular orbital (FMO) analysis, which provides insight into their chemical reactivity and kinetic stability (Table 1). The Highest Occupied Molecular Orbital (HOMO) and Lowest Unoccupied Molecular Orbital (LUMO) energies are critical in understanding the electron-donating and accepting capabilities of the molecules. Among the compounds, Magnoflorine

exhibited the lowest HOMO–LUMO energy gap of 5.01 eV, followed by Tinocordiside (5.13 eV), indicating that these two molecules possess higher chemical reactivity and lower kinetic stability compared to Berberine (5.64 eV) and Palmatine (5.78 eV). A smaller band gap suggests better interaction with biological targets, such as proteins or enzymes, due to easier excitation and electron transition (Parr & Pearson, 1983)[27].

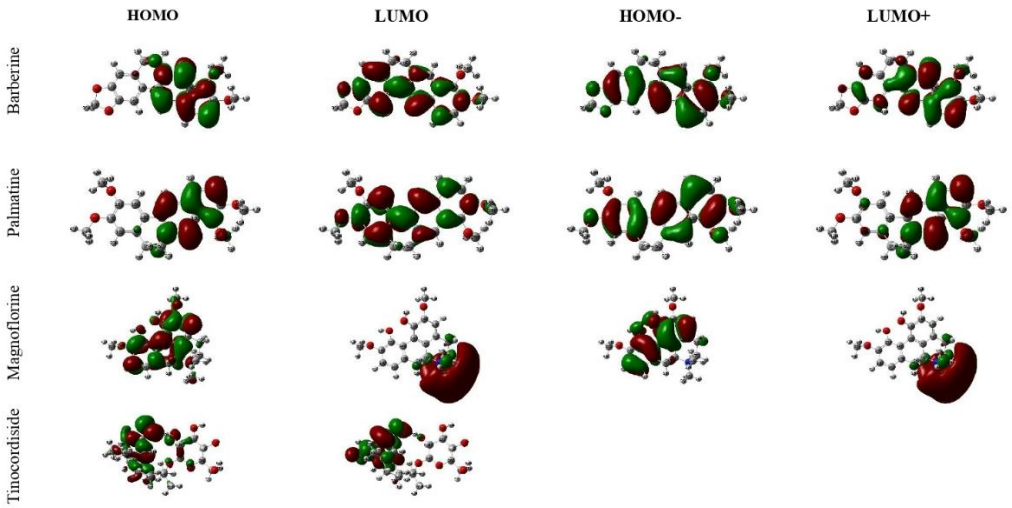

Figure 10. HOMO, LUMO, HOMO-1 and LUMO+ of berberine, palmatine, magnoflorine and tinocordiside.

Furthermore, Tinocordiside had the most negative LUMO energy (–1.66 eV), indicating a strong ability to accept electrons. Its HOMO energy (–6.80 eV) was also the lowest among all, reflecting excellent electron-donating capacity, which is favorable for interactions with electron-deficient receptor sites like EGFR tyrosine kinase. In contrast, Palmatine and Berberine had relatively larger band gaps (5.78 eV and 5.64 eV, respectively), suggesting reduced reactivity**.**

Table 1. HOMO, LUMO and bandgap of all the selected phytochemicals

Sl no	**Sample**	**HOMO (eV)**	**LUMO (eV)**	**Band gap (eV)**
1.	Berberine	-6.32	-0.64	5.64

2.	Palmatine	-6.39	-0.60	5.78
3.	Magnoflorine	-5.28	-0.19	5.01
4.	Tinocordiside	-6.80	-1.66	5.13

The Molecular Electrostatic Potential (MEP) maps of the major phytoconstituents of *T. cordifolia*—berberine, palmatine, magnoflorine, and tinocordiside—were generated and shown in Figure 11, to evaluate their electronic distribution and predict potential interaction sites within the EGFR tyrosine kinase domain. The MEP visualization highlights regions of electron density (red, nucleophilic) and electron deficiency (blue, electrophilic), which are critical in determining the binding affinity and orientation of these molecules in a receptor site.

Berberine exhibited pronounced nucleophilic zones around its methoxy oxygen atoms and moderate electrophilic areas near the aromatic ring and positively charged nitrogen atom. These features suggest that berberine can engage in both hydrogen bonding and electrostatic interactions, particularly with acidic residues such as Asp855 and Glu762 in the EGFR active site. Its planar aromatic structure also makes it favorable for π-π stacking interactions with aromatic residues like Phe856 or Tyr residues within the ATP-binding pocket.

Palmatine, structurally similar to berberine, showed a comparable electrostatic potential map with nucleophilic methoxy groups and an electron-deficient nitrogen center. The subtle differences in potential distribution may result in minor variations in binding orientation or affinity. Like berberine, palmatine is expected to favor hydrophobic, electrostatic, and π-stacking interactions within the EGFR kinase domain, supporting its potential as a competitive inhibitor.

Magnoflorine presented a more dispersed electrostatic profile with strong nucleophilic zones around hydroxyl and methoxy groups and electrophilic features surrounding the

quaternary nitrogen center. Unlike the planar structure of berberine and palmatine, magnoflorine's three-dimensional conformation may allow a more adaptable fit in the binding pocket. Its polar surface suggests the possibility of extensive hydrogen bonding with polar and charged amino acid residues lining the kinase domain.

Tinocordiside, a glycoside, displayed the highest polarity among the four molecules, with multiple hydroxyl groups contributing to dense electron-rich (red) zones across its surface. These regions indicate a strong capacity for hydrogen bonding. However, due to its relatively bulky structure, tinocordiside may not fit easily into the narrow ATP-binding cleft of EGFR but could potentially bind to an adjacent allosteric site or the protein surface, influencing kinase function indirectly through allosteric modulation.

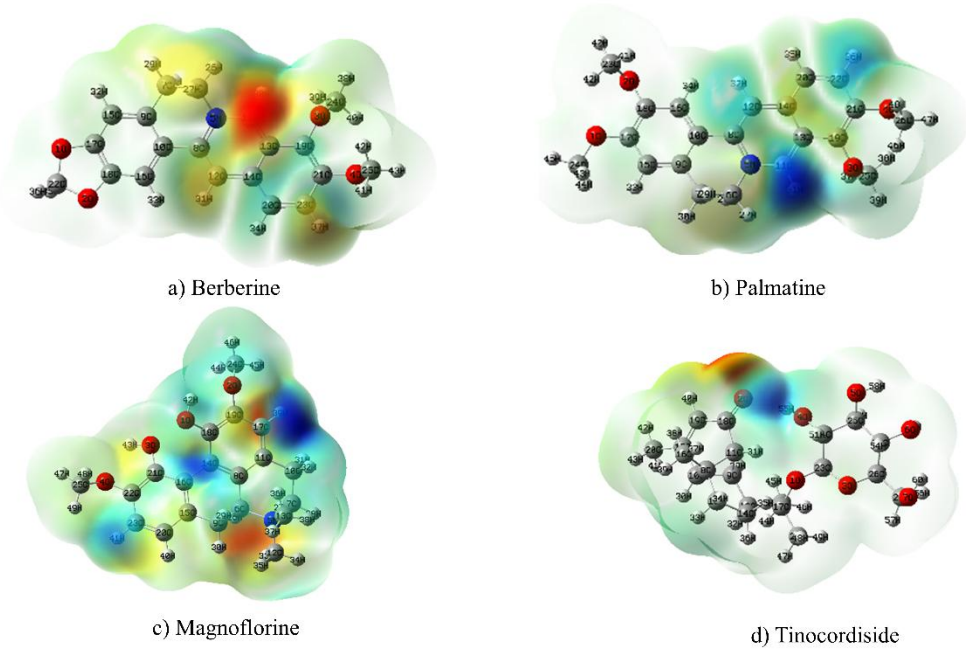

Figure 11. MESP map of of berberine, palmatine, magnoflorine and tinocordiside

To further understand the chemical reactivity and biological potential of the selected natural compounds, global reactivity descriptors such as chemical hardness (η), softness (S), chemical potential (μ), electronegativity (χ), and the electrophilicity index (ω) were calculated using frontier molecular orbital (FMO) energies (Table 2). Among the tested molecules,

Tinocordiside exhibited the highest electrophilicity index (ω = 3.49 eV), which implies a strong tendency to accept electrons. This high value suggests a greater potential for interaction with biological targets, indicating promising biological activity.

In addition, Tinocordiside exhibited the lowest chemical potential (μ = –4.23 eV), indicating its thermodynamic stability and a strong tendency to acquire electrons. This aligns well with its observed moderate chemical softness (S = 0.19 eV^{-1}) and relatively low hardness (η = 2.56 eV), which together support the molecule's chemical reactivity and potential bioavailability. Similarly, Magnoflorine also displayed favorable reactivity characteristics, including a comparable softness (S = 0.19 eV^{-1}) and a slightly lower hardness (η = 2.50 eV). These values indicate a flexible electronic structure that can adapt to biological environments, further enhancing its potential as a bioactive compound. Overall, Tinocordiside stood out due to its balanced profile of high electrophilicity, suitable softness, and stable chemical potential, making it a promising candidate for further pharmacological investigations.

Table 2. Calculated global descriptive parameters for the selected phytochemicals in T.cordifolia

Sample	**Ionization potential (IP)**	**Electron affinity (Ea)**	**Hardness (η)**	**Electro negativity (χ)**	**Softness (S)**	**Chemical potential (μ)**	**Electro Philicity Index (ω)**
Berberine	6.32	0.67	2.82	3.50	0.17	-3.50	2.17
Palmatine	6.39	0.60	2.89	3.49	0.17	-3.49	2.11
Magnoflorine	5.28	0.19	2.50	2.73	0.19	-2.73	1.49
Tinocordiside	6.80	1.66	2.56	4.23	0.19	-4.23	3.49

3.5. Molecular Docking

Molecular docking was employed to investigate the binding interactions of the selected phytoconstituents—Berberine, Palmatine, Magnoflorine, and Tinocordiside—with the EGFR tyrosine kinase domain (PDB ID: 1M17). The inbuilt ligand Erlotinib served as a

reference standard and was redocked using Glide docking to validate the docking protocol. Erlotinib was extracted from the crystal structure of 1M17 and prepared using LigPrep. Glide docking revealed that Erlotinib binds deeply within the active site, forming two hydrogen bonds with ARG 817 and CYS 773. The amino acid residues lining the active site include TYR 777, ASP 776, CYS 773, GLY 772, PHE 771, MET 769, LEU 768, GLN 767, THR 766, LEU 764, VAL 702, LEU 694, ALA 719, ILE 720, LYS 721, CYS 751, MET 742, PHE 832, ASP 831, THR 830, GLU 738, LEU 820, ASN 818, and ARG 817.

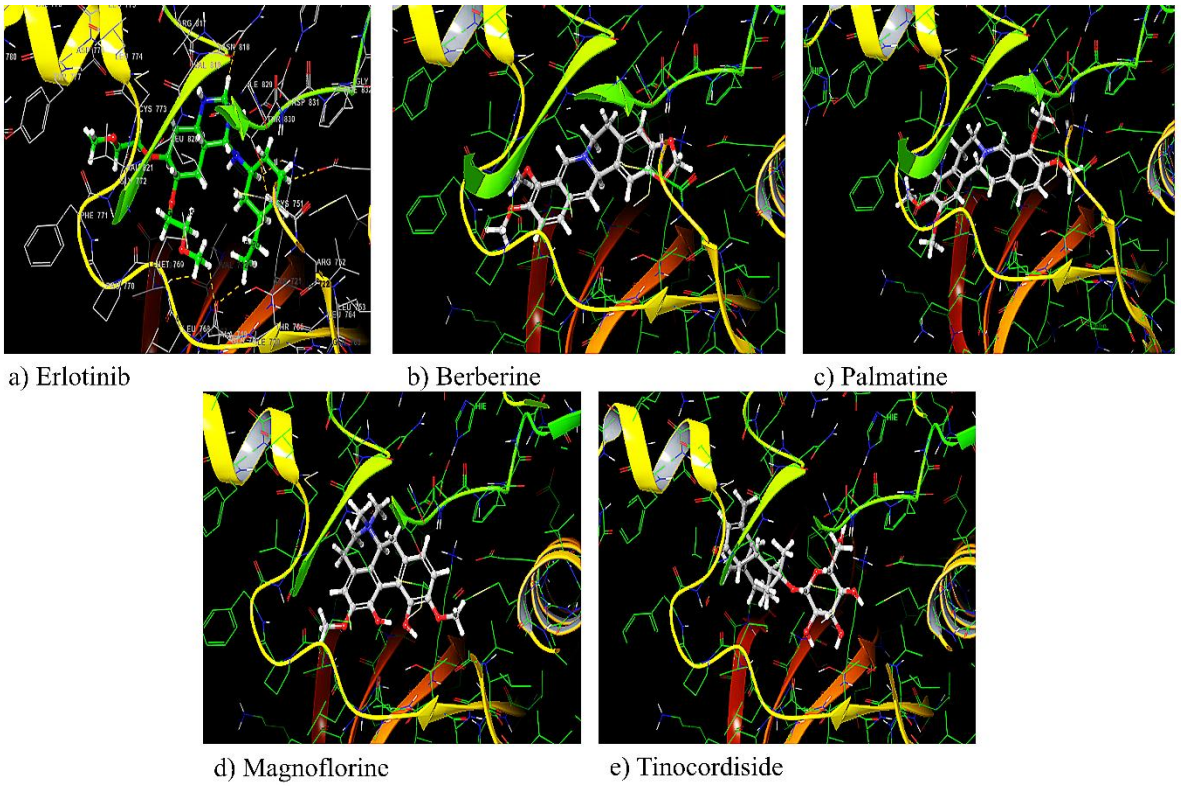

Figure 12. 3D interaction images of inbuilt ligand, erlotinib, and selected phytochemical compounds (berberine, palmatine, magnoflorine, tinocordiside) with EGFR target protein IM17

Berberine was docked into the active site of 1M17 and formed one hydrogen bond with ASP 831. Palmatine was docked into the 1M17 active site without any specific hydrogen bond interaction was observed. Magnoflorine was docked into the same pocket. Similar to Palmatine, Magnoflorine did not form hydrogen bonds with any of the active site residues. Tinocordiside demonstrated the most significant binding interaction among the

phytochemicals. It formed four hydrogen bonds with key residues ASP 831, LYS 721, THR 766, and CYS 773.

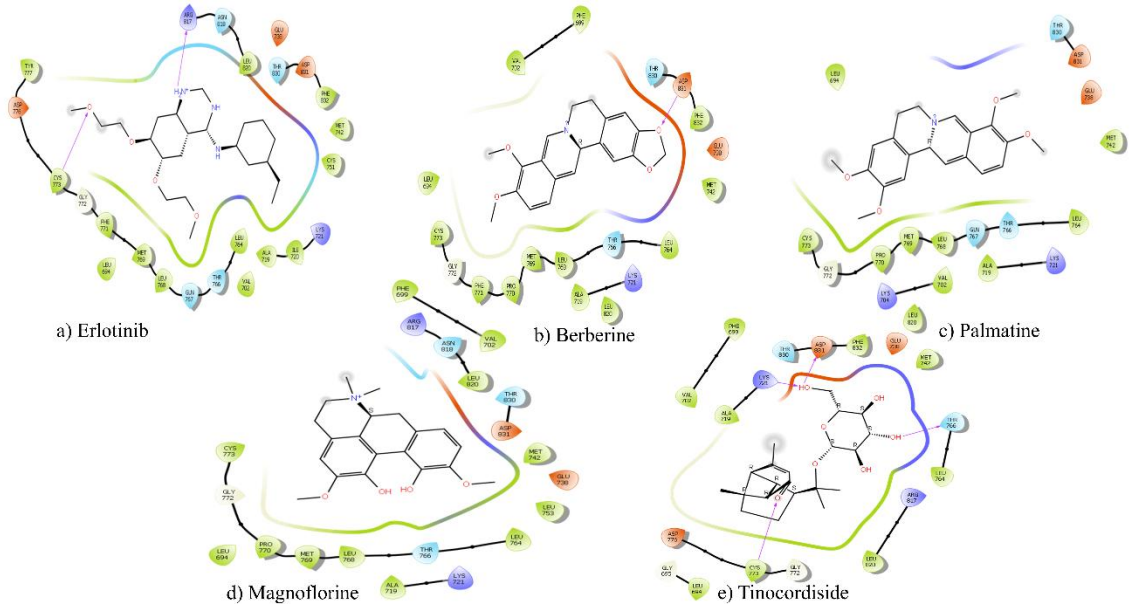

Figure 13. 2D interaction images of inbuilt ligand, erlotinib, and selected phytochemical compounds (berberine, palmatine, magnoflorine, tinocordiside) with EGFR target protein IM17

Erlotinib, the reference ligand, exhibited the highest binding affinity with the lowest glide score of –7.63 kcal/mol, validating the docking procedure. Among the phytoconstituents, Tinocordiside showed the most promising binding affinity (–6.72 kcal/mol), closely approaching that of Erlotinib. Its ability to form four hydrogen bonds suggests a strong and stable interaction with the EGFR active site, underscoring its therapeutic potential.

Although Berberine, Palmatine, and Magnoflorine also showed favorable glide scores (ranging from –4.94 to –5.73 kcal/mol), their binding profiles involved fewer interactions. Notably, Palmatine and Magnoflorine did not form specific hydrogen bonds, potentially reducing their inhibitory efficiency compared to Tinocordiside.These findings support the hypothesis that certain bioactive compounds in *T. cordifolia*—particularly Tinocordiside—may act as EGFR inhibitors, warranting further in vitro and in vivo investigations.

Table 3. Docking score and binding energy of inbuilt ligand, erlotinib, and selected phytochemical compounds (berberine, palmatine, magnoflorine, tinocordiside) with EGFR target protein IM17.

Sl no	Sample	Glide docking score (kcal/mol)	Binding energy (kcal/mol)
1.	Inbuilt ligand (Erlotinib)	-7.63	-40.78
2.	Berberine	-4.94	-37.27
3.	Palmatine	-5.56	-37.48
4.	Magnoflorine	-5.73	-39.25
5.	Tinocordiside	-6.72	-36.35

4. Conclusion

The present study comprehensively evaluated the phytochemical composition, antioxidant potential, cytotoxic efficacy, and molecular interactions of methanolic extract of *T. cordifolia*. FTIR analysis confirmed the presence of diverse functional groups, including amines, hydroxyls, and halogenated compounds, indicative of alkaloids, terpenoids, and phenolic constituents. UV–Vis spectroscopy revealed a strong absorption peak at 290 nm (absorbance: 2.1), correlating with $\pi \rightarrow \pi^*$ transitions of aromatic systems and validating the presence of UV-active phytoconstituents such as berberine and palmatine.

Antioxidant activity assessed via DPPH and hydroxyl radical scavenging assays demonstrated concentration-dependent responses. The DPPH assay yielded an IC_{50} value of 235 µg/mL**,** while hydroxyl radical scavenging activity exceeded 95% inhibition **at** 600 µg/mL, with an IC_{50} also around 235 µg/mL**.** These results underscore the moderate to strong antioxidant potential of the extract.

Cytotoxic assays against EAC and DLA cancer cell lines revealed potent antiproliferative activity. The Trypan blue assay reported IC_{50} values of58.6 µg/mL (EAC) and14.3 µg/mL(DLA), with the extract showing significantly higher efficacy against DLA. The

MTT assay confirmed dose-dependent cytotoxicity, reaching ~53% inhibitionat 300 µg/mL**,** alongside visible morphological changes suggestive of apoptosis or necrosis.

To rationalize these bioactivities, DFT calculations were carried out for four major phytocompounds. Among them, Tinocordiside exhibited the highest electrophilicity index (ω = 3.49 eV**)** and the most negative chemical potential **(**µ = –4.23 eV**),** indicating high reactivity and electron-accepting capacity. Its HOMO–LUMO gap **(**5.13 eV**)** and MEP profile further suggested favorable interactions with biological targets.

Molecular docking studies with EGFR tyrosine kinase (PDB ID: 1M17) validated these predictions. Tinocordiside demonstrated the strongest binding among the phytochemicals, forming four hydrogen bonds (ASP 831, LYS 721, THR 766, CYS 773) and achieving a Glide score of –6.72 kcal/mol**,** closely approaching that of the standard inhibitor Erlotinib **(**–7.63 kcal/mol**).**

In conclusion, *T. cordifolia* methanolic extract demonstrates significant antioxidant and anticancer potential, supported by both in vitro assays and in silico analyses. Tinocordiside, in particular, emerges as a promising lead compound for EGFR-targeted therapies. Further in-depth studies, including mechanistic assays and in vivo validation, are warranted to explore its clinical relevance as a natural anticancer agent.

5. Funding Statement

This research received no specific grant from any funding agency in the public, commercial, or not-for-profit sectors.

6. Declaration Statement

AI tools were used solely for language editing and polishing of the manuscript.

7. Reference

[1] Upadhyay A, Kumar K, Kumar A, Mishra H. Tinospora cordifolia (Willd.) Hook. f. and Thoms. (Guduchi) - validation of the Ayurvedic pharmacology through experimental and clinical studies. Int J Ayurveda Res 2010;1:112. https://doi.org/10.4103/0974-7788.64405.

[2] Singh S, Devi P. Pharmacological potential of Tinospora cordifolia (Willd.) Miers ex hook. & Thoms. (Giloy): A review. J Pharmacogn Phytochem 2017;6:1644–7.

[3] Gupta A, Gupta P, Bajpai G. Tinospora cordifolia (Giloy): An insight on the multifarious pharmacological paradigms of a most promising medicinal ayurvedic herb. Heliyon 2024;10:e26125. https://doi.org/10.1016/j.heliyon.2024.e26125.

[4] Dahiya DP, Subburaju T, Gurav S, Singh SK. Tinospora Cordifolia:- A Review On Its Ethnobotany, Phytochemical & Pharmacological Profile 2011.

[5] Bishayi B, Roychowdhury S. HEPATOPROTECTIVE AND IMMUNOMODULATORY PROPERTIES OF Tinospora cordifolia IN CCl 4 INTOXICATED MATURE ALBINO RATS 2002;27:139–46.

[6] Priya LB, Balasubramanian B, Shanmugaraj B, Subbiah S, Hu RM, Huang CY, et al. Therapeutic Potential of the Medicinal Plant Tinospora cordifolia–Minireview. Phyton-International J Exp Bot 2022;91:1129–40. https://doi.org/10.32604/phyton.2022.017707.

[7] Desai VR, Ramkrishnan R, Chintalwar GJ, Sainis KB. G1-4A, an immunomodulatory polysaccharide from Tinospora cordifolia, modulates macrophage responses and protects mice against lipopolysaccharide induced endotoxic shock. Int Immunopharmacol 2007;7:1375–86. https://doi.org/10.1016/j.intimp.2007.06.004.

[8] Mathew S, Kuttan G. Immunomodulatory and antitumour activities of Tinospora cordifolia. Fitoterapia 1999;70:35–43. https://doi.org/10.1016/S0367-326X(98)00017-3.

[9] Jayaprakash R, Ramesh V, Sridhar MP, Sasikala C. Antioxidant activity of ethanolic extract of Tinospora cordifolia on N-nitrosodiethylamine (diethylnitrosamine) induced liver cancer in male Wister albino rats. J Pharm Bioallied Sci 2015;7:S40–5. https://doi.org/10.4103/0975-7406.155791.

[10] Singh D, Chaudhuri PK. Chemistry and pharmacology of Tinospora cordifolia. Nat Prod Commun 2017;12:299–308. https://doi.org/10.1177/1934578x1701200240.

[11] Dut Jasuja N, Vidyapeeth J. HYPOGLYCEMIC AND ANTIOXIDANT ACTIVITY OF TINOSPORA CORDIFOLIA: A REVIEW Pramod K Raghav 2014.

[12] Chaudhary A, Das R, Mehta K, Mehta DK. Indian herb Tinospora cordifolia and Tinospora species: Phytochemical and therapeutic application. Heliyon 2024;10:e31229. https://doi.org/10.1016/j.heliyon.2024.e31229.

[13] Sakkariya KN, Dev J, Moidu HH. Chemical Profiling, Spectroscopic Characterization thereafter Molecular Docking Studies of Phytochemical Constituents of a Polyherbal Formulation-Biogymnema. Int J Green Herb Chem 2023;12:301–23. https://doi.org/10.24214/ijghc/hc/12/4/30123.

[14] Lekkala VDVV, Muktinutalapati AV, Lebaka VR, Lomada D, Korivi M, Li W, et al. Green Synthesis and Characterization of Silver Nanoparticles from Tinospora cordifolia Leaf Extract: Evaluation of Their Antioxidant, Anti-Inflammatory, Antibacterial, and Antibiofilm Efficacies. Nanomaterials 2025;15. https://doi.org/10.3390/nano15050381.

[15] Palmieri A, Scapoli L, Iapichino A, Mercolini L, Mandrone M, Poli F, et al. Berberine

and Tinospora cordifolia exert a potential anticancer effect on colon cancer cells by acting on specific pathways. Int J Immunopathol Pharmacol 2019;33:1–10. https://doi.org/10.1177/2058738419855567.

[16] Puri A, Patil S. Tinospora cordifolia Stem Extract-mediated Green Synthesis of Selenium Nanoparticles and its Biological Applications. Pharmacognosy Res 2022;14:289–96. https://doi.org/10.5530/pres.14.3.42.

[17] Swami A, Asija DR, Yadav S. Synthesis, characterization and anti-cancer activity of Tinospora cordifolia extract medicated Silver nanoparticles. Int J Pharm Res Dev 2024;6:105–9. https://doi.org/10.33545/26646862.2024.v6.i1a.47.

[18] Puri A, Mohite P, Maitra S, Subramaniyan V, Kumarasamy V, Uti DE, et al. From nature to nanotechnology: The interplay of traditional medicine, green chemistry, and biogenic metallic phytonanoparticles in modern healthcare innovation and sustainability. Biomed Pharmacother 2024;170:116083. https://doi.org/10.1016/j.biopha.2023.116083.

[19] Eng N, Kanagala P, Susmila †, Gaddam A, Gunji P, Kotakadi VS, et al. Synthesis of Bio-Inspired Silver Nanoparticles by Ripe and Unripe Fruit Extract of Tinospora cordifolia and Its Antioxidant, Antibacterial and Catalytic Studies Citation. Nano Biomed Eng 2020;12:214–26. https://doi.org/10.5101/nbe.v12i3.p214-226.

[20] Safna Hussan K, Babu TD, Thayyil MS, T.S S, A A. Physiochemical characterization and Biological evaluation of Amorphous solid dispersions of Erlotinib HCl ; Better Chemotherapeutic Efficacy. Sci Rep 2025;15:1–17.

[21] Kn S, Mv H, Dev J, Tv J, Nk H, Pv MK. Chemical Profiling , Spectroscopic Characterization and Biological Evaluation of a novel polyherbal formulation with natural binders- Ayurgreen Natura Pain Gel 2022;8:72–84.

https://doi.org/10.31254/jahm.2022.8204.

[22] Safna Hussan KP, Babu TD, Pareeth CM, Joshy G, Thayyil MS, Cancer A, et al. Antioxidant activity of erlotinib and gefitinib: theoretical and experimental insights. Free Radic Res 2022;56:196–208.

[23] Devadoss A, Dharmalingam P, Chandraleka S. ORIGINAL ARTICLE Synthesis of silver nanoparticle using Tinospora cordifolia and its characterization and beneficial effects on wastewater treatment 2022:1044–9.

[24] Selvam K, Sudhakar C, Govarthanan M, Thiyagarajan P, Sengottaiyan A, Senthilkumar B, et al. Eco-friendly biosynthesis and characterization of silver nanoparticles using Tinospora cordifolia (Thunb.) Miers and evaluate its antibacterial, antioxidant potential. J Radiat Res Appl Sci 2017;10:6–12. https://doi.org/10.1016/j.jrras.2016.02.005.

[25] Sharma P, Dwivedee BP, Bisht D, Dash AK, Kumar D. The chemical constituents and diverse pharmacological importance of Tinospora cordifolia. Heliyon 2019;5:e02437. https://doi.org/10.1016/J.HELIYON.2019.E02437.

[26] Activity THE, Of A. World Journal of Pharmaceutical 2019;5:88–93.

[27] Samad A, Huq MA, Rahman MS. Bioinformatics approaches identified dasatinib and bortezomib inhibit the activity of MCM7 protein as a potential treatment against human cancer. Sci Rep 2022;12:1–16. https://doi.org/10.1038/s41598-022-05621-0.